Article ID: 1003－6326(2004)05－1017－06

Physical modeling of gas induced bath flow in drained aluminum reduction cell①

LI Xiang-peng(李相鹏), LI Jie(李 劼), LAI Yan-qing(赖延清),
ZHAO Heng-qin(赵恒勤), LIU Ye-xiang(刘业翔)
(School of Metallurgical Science and Engineering, Central South University, Changsha 410083, China)

Abstract: A room temperature physical model was used to study the bubble behavior and gas induced bath circulation in a drained aluminum reduction cell. By passing compressed argon through the penetrated Plexiglas box bottom plate immersed in water, gas evolution at the anode bottom surface was simulated. Bubble behavior and liquid flow field were studied and analysis was presented. Bath secondary recirculation was observed in the interpolar gap not the net rising flow as expected. Liquid driven by the bubbles forms small vortices along the interpolar gap with small mean and turbulent velocities and accordingly poor mass transfer. Secondary recirculation also exists between the slot and interpolar gap, part of the flow in the interpolar gap go to the slot with the bubbles and fluid at the bottom of the slot enters the interpolar gap directly without going to the center channel. The existence of the fluid secondary recirculation is very unfavorable to the alumina dissolution and dispersion. Increasing the anode tilt or gas flow rate, or decreasing the anode-cathode distance can make the secondary recirculation in the interpolar gap weak, however, will intensify the secondary recirculation between the slot and interpolar gap.

Key words: bubble behavior; flow pattern; physical model; drained aluminum reduction cell
CLC number: TF 821 **Document code:** A

1 INTRODUCTION

Hall-Heroult cells (H-H cells) have been used in commercial production for more than one hundred years, and because of their high energy consumption, great efforts have been made to improve the reduction process and save energy. It is already clear that, reduced anode-cathode distance (ACD, $D_{A\text{-}C}$) can work effectively to lower down the cell voltage and energy consumption, however, the interaction of magnetic fields with the current flow in the molten bath and metal pad produces large magnetic forces in the cell, and causes fluctuations of the metal surface and great instability of the electrolysis. To lower down the ACD of the currently used H-H cell would sacrifice the cell stability and result in losses of current efficiency.

A new cell design, called "drained cell", with a sloped cathode and anode was conceived to work well at a shortened interpolar gap. Fig. 1 shows a draft of a typical drained cell design.

From Fig. 1 it can be seen that, there are two symmetric slopes on the cathode, inclining to the center. Anodes with relevant slope hung from the anode beams are configured to match the sloped cathode. The ACD is about 1.5－3.0 cm, and a sump is tcentered in the cell bottom along the side wall. Aluminum deposited on the cathode surface,

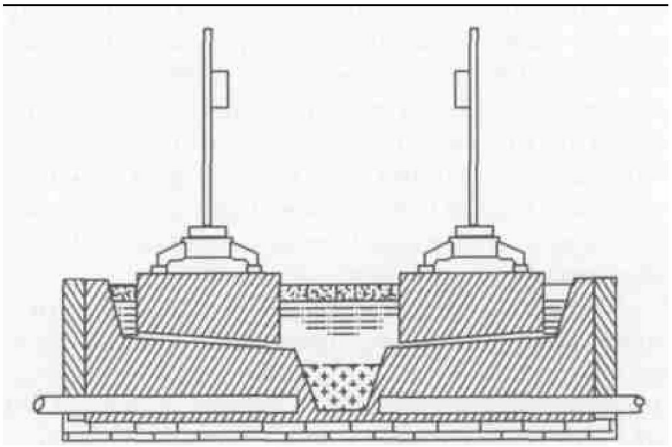

Fig. 1 Schematic representation of drained cell

are drained to the sump, collected there and siphoned timely. Aluminum wettable material, such as TiB_2, is applied as a coating layer on the surface of the cathode, so only a layer of aluminum of about 0.3－0.5 cm is needed to keep good contact between metal pad and cathode, and the aluminum pool with a depth of about 20 cm can be removed[1].

Since 1970s, more and more attentions have been drawn to the drained cell design, and many drained cell designs have been filed as patents[2-7]. From 1987 to 1998, a great deal of work has been done on R& D of the drained cell in Comalco Australia; 25 drained cells were set up and operated at 120

① **Foundation item:** Project(G1999064903) supported by the National Key Fundamental Research and Development Program of China
Received date: 2004－02－23; **Accepted date:** 2004－05－08
Correspondence: LI Xiang-peng, PhD; Tel: +86-731-8830474; E-mail: roclee_xp@163.com

kA, 1.15 A/cm^2 anode current density and 2.5 cm ACD, with an energy consumption of 13 200 kW·h/t[1]. In U.S. drained cell was made one of the top R&D items in the Aluminum Industry Technology Roadmap(2003) by the Department of Energy's Office of Energy Efficiency and Renewable Energy[8]. It is evident that the drained cell technique has attracted extensive interests in many developed countries.

As the ACD of a drained cell is largely decreased, one of the key points of its design is to keep a proper bath circulation, which contributes to the alumina dissolution, mass transfer and the reduction of the concentration and temperature gradients in the cell. Another key point is to keep a workable heat balance. The design of bath flow pattern should guarantee enough alumina transferred to the electrolysis space and meet the need of electrolysis at first, and enough heat transferred to side-ledge and cell wall to keep the cell in a proper heat balance from overheating secondly.

Bath circulation in H-H cells is caused by natural convection, gas induced flow and magnetically induced flow. Theoretical and experimental studies of bath and metal pad circulation have largely been concentrated on the motion induced by magnetic forces in the currently used reduction cells[9-11]. Although such studies have given very valuable insight into flow patterns in metal and bath, the picture is not complete as long as other types of convection are not taken into account[12].

Solheim et al[12] calculated the bath flow in a commercial cell, taking into account the gas induced convection, and the result was in good agreement with the bath flow velocity measured. It was also indicated that the gas induced circulation velocity in the interpolar gap is relatively high, at least of the same magnitude as the magnetically induced convection.

Purdie et al[13] modeled the alumina mixing rate in a cell, and the results showed that predicted mixing rates due to gas driven flow alone had been found to be comparable with the overall measured flow rates. Gas driven flow therefore appeared likely to be a more significant cause of electrolyte mixing than magnetic-hydrodynamics (MHD) driven flow in aluminum reduction cells.

Physical modeling of the gas induced bath circulations in previous work was focused on the bath velocity[12,14], interface waving[15], bath flow pattern and alumina transfer[15] in currently used H-H cells which were characterized by horizontal anode surface and cathode surfaces. Little was known to the gas behavior and bath flow pattern when the anode and cathode are simultaneously sloped, with a largely decreased ACD. Although Solheim[12] studied the evolution of single bubble beneath anodes inclined at various angles to the horizontal, it is still not enough. Totally speaking, scant studies were aimed at the gas driven bath flow fields in a drained cell, but the bubble behavior and the bath flow pattern in it were less clear.

In the present paper, a room temperature water model was used to study the bubble behavior and gas induced bath circulation in a drained cell. The influences of the current density, ACD, inclination of the anode, anode immersion depth on the bubble velocity under anode and the flow pattern were studied quantitatively. The bath viscosity was not considered, since it was studied elsewhere[12] and now has been well understood.

2 EXPERIMENTAL

2.1 Experimental basis

The influence of the anode current density on the gas evolution was modeled by changing the gas flow rate. The gas evolution rate per unit anode surface area Q is in direct ratio to the current density:

$$Q = \frac{JRT}{4Fp} \tag{1}$$

where J is the current density, R is the universal gas constant, T is the absolute temperature, F is the Faraday constant, p is the pressure corresponding to the atmosphere.

The gas flow rate q is determined by the following equation:

$$q = QA \times 10^6$$

where A is the area of the anode bottom surface.

The time used by the a bubble traveling from the evolution point to another fixed point can be used to calculate the gas traveling acceleration a:

$$a = \frac{2S_1}{t^2} \tag{2}$$

where S_1 is the distance from its evolution point to the fixed point, t is the time consumed.

The bubble detaching velocity v can be expressed as:

$$v = \sqrt{2aS_2} \tag{3}$$

where S_2 is the distance from the bubble evolution point to the upper edge of the anode where the bubbles detached.

The time between the evolution of two successive bubbles can be used to calculate the bubble detaching volume V:

$$V = qt_1 \tag{4}$$

where q is gas flow rate, t_1 is the interval of two bubbles evolution.

The subject of similarity between a water model and its prototype has been investigated several times[12,16,17]. It was verified that, as the value of the viscosity and surface tension of water at the room temperature is similar to those of molten bath, the

phenomenon in the liquid should be similar in both cases. So a water model was used here and the most important features of the model cell and industrial cell are listed in Table 1.

Table1 Comparison between water model and industrial cell[12]

Item	Water model	Industrial cell
Bath	Water	Fluoride melt
Metal	No "metal"	Aluminum
Bath temperature/ ℃	20	960
Kinematic viscosity of bath/ ($m^2 \cdot s^{-1}$)	1.5×10^{-6}	$\approx 1.5 \times 10^{-6}$
Kinematic surface tension/ ($m^3 \cdot s^{-2}$)	7.3×10^{-5}	$\approx 6.3 \times 10^{-5}$

2.2 Experimental settings

The experimental settings, including water tank, anode box, parallel cathode plate, rotameter, argon tank, etc, are shown in Fig. 2. The whole physical model was set up according to a 160 kA prebaked cell. Water tank, anode box and the parallel cathode plate were made up of Plexiglas. Anode box was constructed to model half an anode, one side of which was clung to a sidewall of water tank to facilitate the vertical placement of the anode box. 150 tiny holes were evenly distributed on the bottom of the anode box, and by forcing the compressed argon through the holes, gas evolution under the anodes was modeled. The parallel cathode plate was fixed parallel to the anode box bottom with four bolts to model the cathode, and the bolts could be adjusted to change the distance from anode bottom to the plate surface to model the changes of ACD. Under the plate, the syntactic foam was filled, which worked to minimize the impacts of the water system under the plate on the experimental results. The anode box with the parallel plate was fixed to an iron frame and could be rotated to simulate different degrees of anode and cathode inclination. The rotameter connected to the pipe which led to the anode box and argon tank at both ends controlled the gas flow rate.

2.3 Experimental procedure

1) Passed the argon through the rotameter and anode box, and gas flow rate was adjusted, then the bubble velocity and detaching volume were measured.

2) Gas flow rate (q), ACD, the degree of slope (α) and anode immersion depth (h) were changed to simulate different operating conditions.

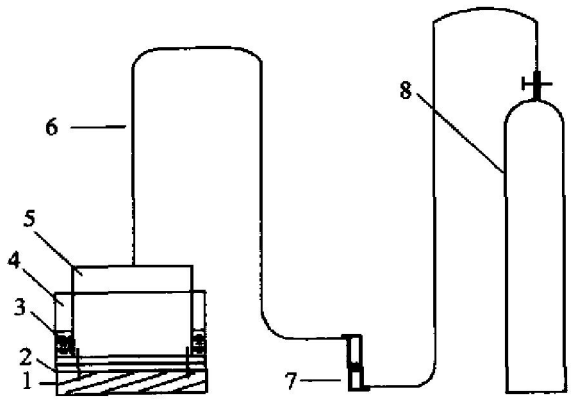

Fig. 2 Experimental settings
1—Syntactic foam; 2—Parallel cathode plate; 3—Water; 4—Water tank; 5—Anode box; 6—Pipes; 7—Rotameter; 8—Argon tank

3) Measurements were conducted after the flow developed undisturbed for 5 min, when each experimental factor was altered, to get a steady state flow in the water tank.

4) Flow tracers such as feathers or dye were added to the fluid, then the flow pattern was observed and fluid velocity in the interpolar gap was measured.

3 RESULTS AND ANALYSIS

3.1 Bubble behavior

Bubbles formed at the bottom of anode and traveled under the slope, majority of them (> 90%) traveled along the entire length of the anode and released at the upper edge of the slope, and the rest would enter the slot, which represents the channel between two anodes. Some small bubbles would coalesce to a bigger one as they traveled along the slope, bigger bubbles attained higher terminal velocities than the small ones, and this caused some bubbles to collide with others and amalgamated together, attaining still higher terminal velocities until they detached from the edge of the anode.

Fig. 3 shows the measured velocity variation with the changes of ACD. Three zones were evident. In zone I, ACD was less than 2.0 cm, and the bubble velocity increased relatively slowly; when entered zone II, as ACD increased, bubble velocity would increase fast, and there was a tendency that the velocity would increase more rapidly as the anode bottom slope increased; when ACD was more than 4 cm, the bubble velocity increase would slow down as seen in zone III

Fig. 4 gives the trend of bubble velocity increased with the anode bottom slope increasing. We can see

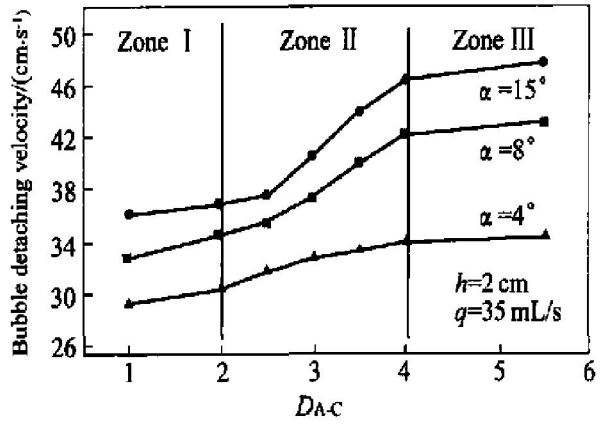

Fig. 3 Effect of ACD on bubble detaching velocity

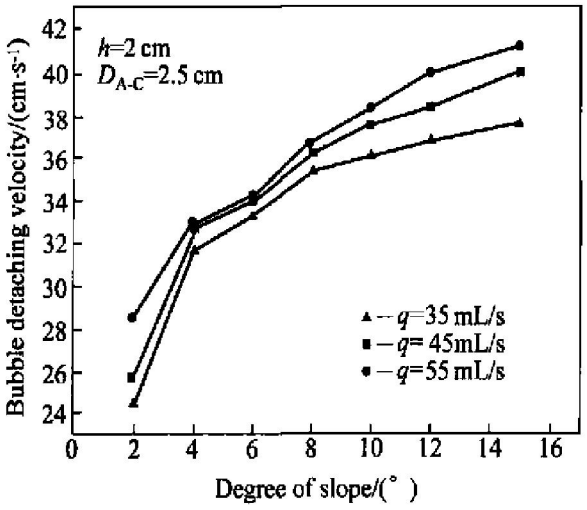

Fig. 4 Effect of anode tilt on bubble detaching velocity

that as the degree of anode bottom slope increased, the bubble velocity increased consistently, however, as the slope was more than 4°, bubble velocity increased slowly.

No apparent influence was found of the anode immersion depth on the bubble velocity in the experiments, as shown in Fig. 5. The result showed that when the anode immersion depth increased from 1.5 cm to 2.5 cm, the bubble velocity slightly changed.

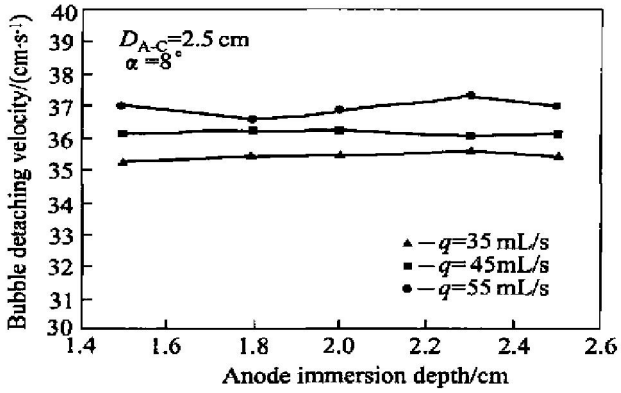

Fig. 5 Effect of anode immersion depth on bubble detaching velocity

From Fig. 4 and Fig. 5, it also can be seen that, the bubble velocity would increase when the gas flow rate increased.

The bubble detaching volume is in relation to the bubble residence time and percentage of anode bottom area covered by bubbles, which contributes significantly to the overall resistance in the interpolar gap studied as a function of anode inclination angle. Fig. 6 shows that the bubble volume necessary for detachment decreased with the increase of inclination angle, which means that as the slope increased, the bubble residence time shortened. The experiment results also indicated that the bubble detaching volume increased with the increase of gas flow rate. Previous work[9] announced that the bubble residence time would decrease fast with the increment of ACD when it was less than 3 cm, and increase slowly when it was more than 3 cm.

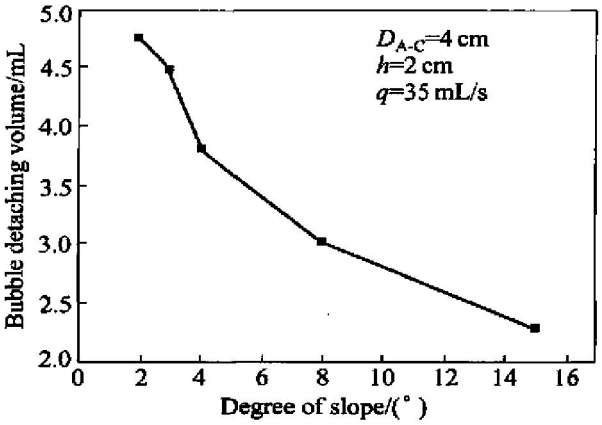

Fig. 6 Effect of anode tilt on bubble detaching volume

3.2 Flow pattern of liquid

The traveling of bubbles dragged the adjacent liquid to move, and formed a flow field around the anode. In order to obtain the water velocity in the interpolar gap, the time of the water traveling through two fixed points was measured. When conducting the measurements, ACD was adjusted to 2.5 cm. Because of the turbulence, the measurements was only conducted when the gas flow rate was 35 mL/s (relevant current density was 0.7 A/cm^2).

Then the average velocities between the two points were calculated according to the time measured and with the change of the anode tilt as shown in Fig. 7.

From Fig. 7 it can be seen that the fluid velocity in the interpolar gap increased with the increase of the anode tilt, however the anode immersion depth had little influences on it.

Fluid flow pattern was observed through adding dye or feathers to the liquid at the position of presumed alumina feeding point. A sketch of the resulting flow field in three dimensions is shown in Fig. 8.

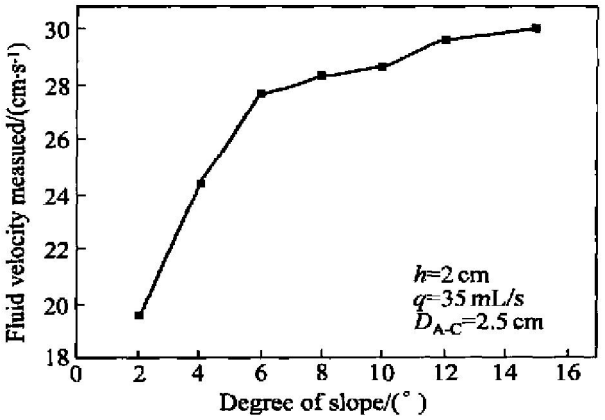

Fig. 7 Effect of anode tilt on fluid velocity in interpolar gap

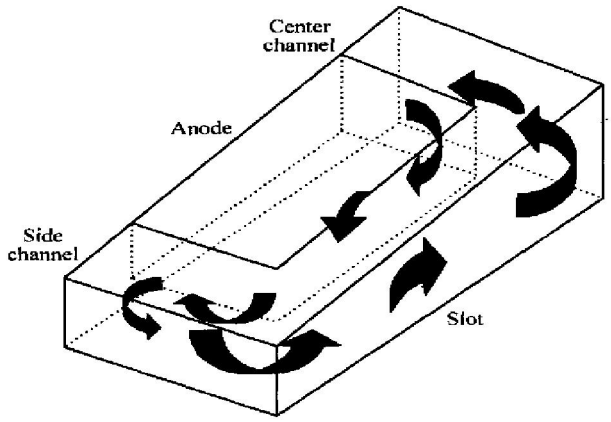

Fig. 8 Liquid flow pattern around an anode

The fluid driven by the bubbles rushed into the side channel, through the slot went to the center channel, then turned downward and returned to the interpolar gap again. In the interpolar gap, liquid close to the anode bottom moved at a high speed, which was likely the same as that of the bubbles, and formed a upper layer of rising flow, while the liquid near the parallel cathode plate, was nearly stagnant. One interesting phenomenon should be noted that, in spite of the net rising flow in the interpolar gap, secondary recirculation flow was observed. The liquid driven by the bubbles formed vortices along the interpolar gap with small mean and turbulent velocities and accordingly poor mass transfer; some liquid entering the side channel from the interpolar gap would return to the interpolar gap at the bottom of the side channel, forming a layer of returning flow under the upper rising flow. Bubbles escaped to the side channel, causing great turbulence there. Drastic turbulence was also observed in the slot, and a small portion of the fluid emerged from the interpolar gap at the side of the anode directly into the slot with the bubbles, then traveled along the slot with the flow from the side channel in large vortices to the center channel. Some of the liquid in slot entered the interpolar gap again with vortices without entering the center channel. So another fluid secondary recirculation was formed between the slot and interpolar gap which was relatively bigger than that of the interpolar gap. The liquid flow in the center channel was less turbulent.

In a running aluminum reduction cell, when adding alumina to the bath, it is important to attain high mixing and transfer speed, however, the observed secondary recirculation in the fluid was almost unfavorable. It was found in the experiments that increasing the anode immersion depth could reduce the liquid secondary recirculation, and the flow in the side channel and slot became less turbulent. When the slope or gas flow rate increased, the liquid velocity in the interpolar gap increased fast. Liquid flow became more turbulent, and the fluid recirculation in the interpolar gap decreased. As the ACD decreased, the liquid recirculation in the interpolar gap became weak. No recirculation flow was found in the interpolar gap when the ACD was reduced to 1 cm. Increasing the slope or gas flow rate, or reducing the ACD would intensify the fluid recirculation between the slot and interpolar gap.

4 CONCLUSIONS

A half anode-water tank physical model was set up to study the bubble behavior and bath flow pattern in a drained cell, showing that water modeling was a useful tool for investigating these phenomena.

Bubble behavior variations with ACD, anode tilt, current density and anode immersion depth were studied. Fluid field is observed, and because of the bubble discharging, great turbulence is found in the side channel and slot. The most important phenomenon observed in the liquid is the existence of the fluid secondary recirculation in the slot and interpolar gap, which was disadvantageous to the dissolution and dispersion of alumina. Increasing the anode tilt or gas flow rate, or decreasing the ACD, the fluid secondary recirculation will be weakened in the interpolar gap, while will be strengthened between the slot and interpolar gap.

REFERENCES

[1] Brown G D, Hardie G J, Shaw R W, et al. TiB_2 coated aluminium reduction cells: status and future direction of coated cell in Comalco[A]. Welch B. Aluminium Smelting Conference[C]. Queenstown, New Zealand, 1998. 529 - 538.

[2] Vittorio de Nora. Cell for Aluminium Electrowinning Employing a Cathode Cell Bottom Made of Carbon Blocks Which have Parallel Channels Therein[P]. United States Patent 683559, 1997.

[3] Stedman I G, Houston G J, Shaw R W, et al. Aluminum Smelting Cells [P]. United States Patent 5043047, 1991.

[4] de Nora V. (Nassau, BS): Cell for Aluminum Electrowinning[P]. United States Patent 6093304, 2000.
[5] Sierre G B(CH): Aluminum Production Cell and Cathode [P]. United States Patent 6358393, 2002.
[6] de Nora V, Bahamas S H, Duruz J J. Cell for Electrolysis of Alumina at Low Temperatures[P]. United States Patent 5725744, 1998.
[7] de Nora V(Nassau, BS), Jean-Jacques D(Geneva, CH). Porous Non-carbon metal-Based Anodes for Aluminum Production Cells[P]. United States Patent 6113758, 2000.
[8] Office of Energy Efficiency and Renewable Energy OF USA, Aluminum Industry Technology Roadmap[EB/OL]. http://www.oit.doe.gov/aluminum, 2003. 2.
[9] Urata N, Arita Y, Ikeuchi H. Magnetic field and flow pattern of liquid aluminum in the reduction cells[A]. Light Metals[C]. Warrendale, PA, USA, TMS, 1975. 233-250.
[10] Wahnsiedler W E. Hydrodynamic modeling of commercial Hall-Heroult cells[A]. Light Metals[C]. Warrendale, PA, USA, TMS, 1988. 269-273.
[11] Tarapore E D. Magnetic fields in aluminum reduction cells and their influence on metal pad circulation[A]. Light Metals[C]. Warrendale, PA, USA, TMS, 1979. 541-550.
[12] Solheim A, Johansen S T, Rolseth S, et al. Gas driven flow in Hall-Heroult cells[A]. Light Metals[C]. Warrendale, PA, USA, TMS, 1989. 245-252.
[13] Purdie J M, Bilek M, Taylor M P, et al. Impact of anode gas evolution on electrolyte flow and mixing in aluminum electrowinning cells[A]. Light Metals[C]. Warrendale, PA, USA, TMS, 1993. 355-360.
[14] Dernedde E. Gas induced circulation in an aluminum reduction cell[A]. Light Metals[C]. Warrendale, PA, USA, TMS, 1975. 111-122.
[15] Chessonis D C, Lacamera A F. The influence of gas-driven circulation on alumina distribution and interface motion in a Hall-Heroult cell[A]. Light Metals[C]. Warrendale, PA, USA, TMS, 1990. 211-219.
[16] Fortin S, Gerhardt M, Gesing A J. Physical modeling of bubble behavior and gas release from aluminum reduction cell anodes[A]. Light Metals[C]. Warrendale, PA, USA, TMS, 1984. 721-741.
[17] Shekhar R, Evans J W. Modeling studies of electrolyte flow and bubble behavior in advanced Hall cells[A]. Light Metals[C]. Warrendale, PA, USA, TMS, 1990. 243-248.

(Edited by YANG Bing)